Supplemental data

A Salt-Induced Reno-Cerebral Reflex Activates RAS and Promotes CKD Progression

Running Title: Reno-Cerebral reflex in CKD

Wei Cao,* Aiqing Li,* Liangliang Wang,* Zhanmei Zhou,* Zhengxiu Su,* Wei Bin,* Christopher S. Wilcox,† and Fan Fan Hou*

*State Key Laboratory of Organ Failure Research, National Clinical Research Center of Kidney Disease, Nanfang Hospital, Southern Medical University, Guangzhou 510515, P. R. China, †Hypertension, Kidney and Vascular Research Center, Georgetown University, Washington, District of Columbia, USA.

Authorship note: Wei Cao and Aiqing Li contributed equally to this work

Correspondence: Dr. Fan Fan Hou, Division of Nephrology, Nanfang Hospital, 1838 North Guangzhou Avenue, Guangzhou 510515, P. R. China. Phone: 86-20-61641591; Fax: 86-20-87281713; E-mail: ffhouguangzhou@163.com.

Total number of figures: 6

Total number of tables: 1

METHODS

Animals

Five-week-old male Sprague-Dawley rats (Nanfang Hospital Animal Experiment Center) were maintained in a pathogen-free facility under controlled temperature (24±2°C) and humidity (55±5%), with a 12-hour light/dark cycle. All animal experiments were approved by the Animal Ethics Committee of Nanfang Hospital.

Animal Treatments

Protocol 1. Five-sixths nephrectomy (5/6Nx) or sham operation (sham) was performed at 6 weeks of age as previously described.[1] After operation, all rats received normal-salt diet for eight weeks, and then were randomly assigned to three groups (n=6 per group) receiving low-salt (0.02% NaCl), normal-salt (0.4% NaCl), or high-salt (4% NaCl) diet (Trophic Animal Feed High-tech Co., Ltd) for 2 weeks.

Protocol 2. 5/6Nx rats were fed with a high-salt (4% NaCl) diet for two weeks and randomly assigned to 12 groups matched for body weight and serum creatinine level (n=6 in each group). They received the following treatments for 2 weeks: (1) IG vehicle (PBS, pH 7.4) or losartan (Sigma Chemical) at 1, 50, or 500 mg/kg/d (group 1-4); (2) ICV vehicle (artificial cerebrospinal fluid) or losartan at 1mg/kg/d using an Alzet osmotic minipump (Durect Corp)[2] (group 5&6); (3) ICV clonidine (Sigma Chemical) at 5.76 μg/kg/d using an osmotic minipump (group 7); (4) Renal denervation as previously described[3] (group 8); (5) selective dorsal rhizotomy as previously described[4] (group 9); (6) ICV tempol at (4.5 μg/kg/d) using an osmotic minipump (group 10); (7) IG tempol at 30mg/kg/d (group 11); (8) IG hydralazine (Sigma Chemical) at 15mg/kg/d (group 12).

The doses of ICV losartan, clonidine or tempol were chosen according to the preliminary studies in which intravenous injection of the doses had no detectable effect on Ang II-induced

increase in BP or renal norepinephrine levels. The accuracy of the ICV injection was confirmed by using the tracer Evans blue. The dose of IG tempol (1–6 mmol/l) corrected parameter of oxidative stress in published studies of hypertension without evidence of dose dependency across this range.[5] The dose of hydralazine was chosen to reduce the BP similarly to rats given ICV losartan.

Renal denervation was performed as described previously.[3] Left flank incision was made, and renal denervation was performed by surgically stripping the renal arteries and veins of adventitia, cutting all visible renal nerve bundles under a dissection microscope (×25). Renal vessels were painted with 10% phenol in an alcohol solution to ensure the destruction of any remaining nerves. Completeness of renal denervation was demonstrated by reduction of renal norepinephrine content less than 5% of control.

Dorsal rhizotomy was performed according to previous reports.[4,6] A dorsal incision was made and the thoracic and lumbar vertebral eolumn exposed by gently pulling the museulature away from the vertebrae. Then, the left vertebral laminae from T10 to L3 were removed with small bone scissors. Under a dissecting microscope, the dura was opened directly over the left dorsal root entry zone from T10 to L3 and the left dorsal roots were cut near their zone of entry by angled microscissors. All rats receiving dorsal rhizotomy survived without paralysis of the legs or bladder.

Measurement of SBP and Renal Function

PE-50 catheters were inserted into the femoral artery under isoflurane anesthesia to measure SBP using a pressure transducer (Gould) connected to a physiologic recorder (Gilson Medical Electronics).[1]

Serum creatinine and sodium concentration were measured with an automatic chemistry analyzer (AU480, Beckman Coulter) and urinary albumin with an ELISA kit (IMTEC

Diagnostics). Values were averaged over 3 consecutive days.

Histological Evaluation

Evaluation of Renal Fibrosis

Histological analysis. Animals were anesthetized with sodium pentobarbital (50mg/kg) and perfused *via* an intracardiac cannula with ice-cold PBS followed by ice-cold 4% paraformaldehyde (Sigma Chemical) in PBS. The kidneys were dissected and fixed in 4% paraformaldehyde in PBS overnight at 4 °C. Two-micrometer-thick sections were processed for periodic acid-Schiff (PAS, for evaluation of glomerulosclerosis) and Masson's trichrome staining (MT, for evaluation of tubulointerstitial fibrosis). The extent of renal fibrosis was quantitated under a light microscope as previously described.[1]

Immunohistochemistry Analysis. Five-micrometer-thick sections were processed[7] using anti-rat fibronectin (1:200, Sigma Chemical) and anti-rat collagen I (1:100, Millipore). Intrarenal expression of fibronectin and collagen I were semi-quantitated as described previously.[8] Briefly, digital images (at 1360×1024 pixel resolution) of 10 randomly selected tubulointerstitial areas were captured at 400 × magnification by a DP 71 CCD camera (Olympus) coupled to an Olympus AX-70 microscope (Olympus). The staining scores were calculated by Image-Pro Plus software (version 6.0, Media Cybernetics). Data were expressed as the ratio of integrated optical density (IOD) to observed area (IOD/area).

Western Blot. The protein levels of fibronectin and collagen I in homogenates of renal cortex were determined as described[9] with anti-rat fibronectin and collagen I antibodies.

Real-Time PCR. Renal mRNA levels of fibronectin and collagen I were analyzed by real-time RT-PCR.[10] The levels of mRNA were normalized to GAPDH.

Evaluation of Renal Macrophage Infiltration

Kidneys were stained with a monoclonal antibody (1:50) specifically recognizing

macrophage marker ED-1 (Serotec, Inc.). Macrophage infiltration was quantified by counting the ED-1-positive cells in 20 randomly chosen glomerular profiles and in 20 (0.3×0.3 mm^2) tubulointerstitial areas.

Cerebral Neuronal Activation

This was assessed in forebrain nuclei by using c-fos expression as a functional marker. Animals were anesthetized and perfused as described above. Whole brain was dissected and cut into thick coronal slices (2 mm) with a rat brain slicer matrix (Zivic Instruments). Slices were post-fixed overnight at 4°C in 4% paraformaldehyde, embedded in paraffin, and cut into two-micrometer serial thick sections. Forebrain nuclei were identified under a microscopy and immunohistochemical staining was performed to determine c-fos positive cells in the nuclei using an anti-c-fos antibody (Millipore). Bright-field images were captured using an Olympus upright microscope (BX51, Olympus). The number of c-fos positive cells was counted in three sections from each part of the brain using Image-Pro Plus software and results expressed positive cells per $10^4\mu m$.[11]

All histological analyses were performed by two pathologists who were blinded to the treatment of the animals.

RAS Expression and Activity

Expression of RAS Components in Kidney

Immunohistochemistry Analysis. Five-micrometer-thick sections were processed[7] using: anti-rat AGT (1:200, IBL), anti-rat ACE-1 (1:100, Santa Cruz), anti-Ang II (1:800, Peninsula Laboratories), anti-rat AT1 receptors (1:100, Millipore), and anti-rat renin (1:50, Santa Cruz) antibodies and intrarenal expression was semi-quantitated as described above.

Intrarenal renin was assessed as described previously.[12] The renin-positive JGAs were identified by immunohistochemical staining using anti-renin antibody (Santa Cruz). Renin

expression was expressed as the renin-positive JGA/total JGA x 100 (%JGA). The % JGA obtained for each section was pooled and averaged for each animal. Comparisons were made using the final % JGA obtained for each animal. Only JGAs with a clearly identified vas afferens entering the glomerulus were used for computation.

Western Blot. The levels of RAS components in homogenates of renal cortex were determined as described previously[9] using: anti-AGT (IBL), anti-ACE-1 (Santa Cruz), anti-AT1 receptors (Millipore), and anti- -actin (Cell Signaling Technology) antibodies.

mRNA Expression of RAS. Renal mRNA levels of AGT, ACE-1, and AT1 receptors were analyzed by real-time RT-PCR as previously described[7] and were normalized to GAPDH.

Localization of Intrarenal RAS. Intrarenal localization of RAS components was determined with double-staining immunohistochemistry on 5 μm paraffin-embedded sections that were dewaxed and microwaved (100°C) in 10 mM citrate buffer (pH 6.0) for 5 min to unmask the antigen. After blocking the endogenous peroxides, the sections were incubated at 4°C overnight with the first primary antibodies against AGT (1:100, IBL), ACE-1 (1:100, Santa Cruz), Ang II (1:800, Peninsula Laboratories), and AT1 receptors (1:200, Millipore), separately, and visualized by diaminobenzidine (DAB) using the EnVision Doublestain Detection Kit (Dako). The sections were washed and incubated at 4°C overnight with the second primary antibodies against the markers of tubular epithelial cells: anti-aquaporin 1 (AQP-1, a marker of proximal tubular epithelial cells; 1:100, Abcam); anti-Tamm-Horsfall protein (THP, a marker of thick ascending limbs of Henle; 1:100, Santa Cruz); anti-thiazide-sensitive NaCl cotransporter (NCCT, a marker of distal convoluted tubular epithelial cells; 1:500, Millipore); anti-aquaporin 2 (AQP-2, a marker of collecting duct epithelial cells; 1:100, Novus) antibody, separately. The slides were visualized by alkaline phosphatase using EnVision Doublestain Detection Kit (Dako). All sections were counterstained with hematoxylin.

Activity of RAS in Kideny and Circulation

Level of RAS Components. Plasma levels of AGT were assessed with an ELISA kit (IBL). Concentrations of Ang II in plasma and renal cortex homogenates were assessed by a competitive ELISA (Peninsula Laboratories). Urinary AGT was assessed by ELISA (IBL).

Activity of Renin and ACE-1. Plasma renin activity was determined by a radioimmunoassay kit (SRL). Serum and renal cortex hemogenates for ACE-1 activity were analyzed by a fluorometric method and normalized for protein content determined by a BCA Protein Assay Kit (Pierce).[13-14]

Expression of RAS in Brain

Immunohistochemistry and Real-Time RT-PCR. The cerebral expression of Ang II and AT1 receptors were quantitated as described for c-fos analysis. AT1 receptors expression also was analyzed with RT-PCR in homogenates of forebrain nuclei obtained by micropunching using a 0.5-mm-diameter stainless steel needle under a stereoscope (SZX2-ILLB, Olympus).

Localization of Brain RAS. Cerebral localization of Ang II and AT1 receptors were determined by double-staining immunofluorescence,[8] using anti-Ang II or anti-AT1 receptors as the first primary antibody, and anti-GFAP (Millipore) or anti-NSE (Millipore) as the second primary antibody.

Evaluation of Sympathetic Activity

Norepinephrine Concentrations

Concentrations of norepinephrine in plasma and renal cortex homogenates were assessed with an ELISA kit (ALPCO Diagnostics)[3] according to the manufacturer's protocol.

Expression of TH in Brain

Expression of TH in forebrain nuclei was analyzed by using western blot.[11] Samples frozen in liquid nitrogen were cut into 200-μm coronal sections and specific forebrain nuclei

were obtained as described above. Expression of TH in nuclei homogenates was determined by western blot using an anti-TH antibody (Abcam).[11]

The number of c-fos-positive and TH-expressing neurons in the RVLM was determined as previously described.[15] Briefly, brain stem sections were double stained with antibodies against TH (Milipore) and c-fos (Santa Cruz) and the number of labeled TH and c-fos immunopositive neurons located within the defined borders of the RVLM as delineated in the atlas of Paxinos and Watson.

Evaluation of Oxidative Stress

Expression of NADPH Oxidase Subunits in Renal Cortex

The levels of NADPH oxidase subunits Nox2 and Nox4 in homogenates of renal cortex were determined[9] using anti-Nox2 and anti-Nox4 antibodies (Santa Cruz).

Expression of NADPH Oxidase Subunits in Brain

Brain samples frozen in liquid nitrogen were cut into 200-μm coronal sections and specific forebrain nuclei were obtained as described above. Expression of Nox2 and Nox4 were determined by western blot using anti-Nox2 and anti-Nox4 antibodies (Santa Cruz).[11]

Statistic Analyses

All data are expressed as mean ± SD of three independent experiments. Continuous variables between groups were compared using one-way ANOVA, followed by LSD test. Statistical analyses were conducted with SPSS 17.0 for Windows (SPSS). A value of $P<0.05$ was considered statistically significant.

REFERENCES

1. Li HY, Hou FF, Zhang X, Chen PY, Liu SX, Feng JX, Liu ZQ, Shan YX, Wang GB, Zhou ZM, Tian JW, Xie D: Advanced oxidation protein products accelerate renal fibrosis in a remnant kidney model. *J Am Soc Nephrol* 18: 528-538, 2007
2. Huang BS, Leenen FH: Both brain angiotensin II and "ouabain" contribute to sympathoexcitation and hypertension in Dahl S rats on high salt intake. *Hypertension* 32: 1028-1033, 1998
3. Veelken R, Vogel EM, Hilgers K, Amann K, Hartner A, Sass G, Neuhuber W, Tiegs G: Autonomic renal denervation ameliorates experimental glomerulonephritis. *J Am Soc Nephrol* 19: 1371-1378, 2008
4. Ye S, Ozgur B, Campese VM: Renal afferent impulses, the posterior hypothalamus, and hypertension in rats with chronic renal failure. *Kidney Int* 51: 722-727, 1997
5. Wilcox CS, Pearlman A: Chemistry and antihypertensive effects of tempol and other nitroxides. *Pharmacol Rev* 60: 418-469, 2008
6. Pan JY, Bishop VS, Ball NA, Haywood JR: Inability of dorsal spinal rhizotomy to prevent renal wrap hypertension in rats. *Hypertension* 7: 722-728, 1985
7. Cao W, Xu J, Zhou ZM, Wang GB, Hou FF, Nie J: Advanced oxidation protein products activate intrarenal renin-angiotensin system via a CD36-mediated, redox-dependent pathway. *Antioxid Redox Signal* 18: 19-35, 2013
8. Xavier LL, Viola GG, Ferraz AC, Da Cunha C, Deonizio JM, Netto CA, Achaval M: A simple and fast densitometric method for the analysis of tyrosine hydroxylase immunoreactivity in the substantia nigra pars compacta and in the ventral tegmental area. *Brain Res Brain Res Protoc* 16: 58-64, 2005
9. Cao W, Zhou QG, Nie J, Wang GB, Liu Y, Zhou ZM, Hou FF: Albumin overload activates intrarenal renin-angiotensin system through protein kinase C and NADPH

oxidase-dependent pathway. *J Hypertens* 29: 1411-1421, 2011

10. Xiao HB, Liu RH, Ling GH, Xiao L, Xia YC, Liu FY, Li J, Liu YH, Chen QK, Lv JL, Zhan M, Yang SK, Kanwar YS, Sun L: HSP47 regulates ECM accumulation in renal proximal tubular cells induced by TGF-beta1 through ERK1/2 and JNK MAPK pathways. *Am J Physiol Renal Physiol* 303: F757-765, 2012
11. Jo H, Yang EK, Lee WJ, Park KY, Kim HJ, Park JS: Gene expression of central and peripheral renin-angiotensin system components upon dietary sodium intake in rats. *Regul Pept* 67: 115-121, 1996
12. Pupilli C, Chevalier RL, Carey RM, Gomez RA: Distribution and content of renin and renin mRNA in remnant kidney of adult rat. *Am J Physiol* 263: F731-738, 1992
13. Friedland J, Silverstein E: A sensitive fluorimetric assay for serum angiotensin-converting enzyme. *Am J Clin Pathol* 66: 416-424, 1976
14. Fabris B, Candido R, Carraro M, Fior F, Artero M, Zennaro C, Cattin MR, Fiorotto A, Bortoletto M, Millevoi C, Bardelli M, Faccini L, Carretta R: Modulation of incipient glomerular lesions in experimental diabetic nephropathy by hypotensive and subhypotensive dosages of an ACE inhibitor. *Diabetes* 50: 2619-2624, 2001
15. Yao ST, May CN: Intra-carotid angiotensin II activates tyrosine hydroxylase-expressing rostral ventrolateral medulla neurons following blood-brain barrier disruption in rats. *Neuroscience* 245: 148-156, 2013

Supplemental Figure Legends

Supplemental Figure 1. High salt induces extracellular matrix accumulation in 5/6Nx rats. (A-D) High-salt intake increases expression of fibronectin (FN) and collagen I (Co I) in 5/6Nx rats: representative photos of FN and Co I expression (A), quantitative analysis of extracellular matrix expression (B), expression of FN and Co I at protein (C) and mRNA (D) levels. (E-G) Central administration of losartan or tempol and RDX or SDR inhibit salt-induced extracellular accumulation in 5/6Nx rats: representative photos of immunohistochemical staining for FN and Co I (E), semi-quantitative data (F), and expression of FN and Co I measured by western blot (G). (H) Blood pressure in high-salt-fed 5/6Nx rats treated with indicated intervention approaches.

Supplemental Figure 2. High-salt intake activates intrarenal RAS in 5/6Nx rats. (A) Expression of RAS mRNA in renal cortex. (B) Expression of RAS protein in renal cortex. (C) The activity of ACE-1 in renal cortex. (D) The level of Ang II in renal cortex. (E) Urinary AGT excretion. Data from 3 independent experiments are expressed as mean ± SD (n=6 in each group). *P<0.05 *vs* normal salt in the respective group.

Supplemental Figure 3. High-salt intake unregulates expression of central RAS in brain organum vasculosum laminae terminalis and supraoptic nucleus in 5/6Nx rats. (A) Expression of RAS components in organum vasculosum laminae terminalis (OVLT): representative photos of immunohistochemistry staining (A1) and semi-quantitative data (A2). (B) Expression of RAS components in supraoptic nucleus (SON): representative photos of immunohistochemistry staining (B1) and semi-quantitative data (B2). (C) Expression of AGT and ACE-1 in subfornical organ (SFO): representative photos of immunohistochemistry staining (C1) and semi-quantitative data (C2). (D) Expression of AGT and ACE-1 in

paraventricular nucleus (PVN): representative photos of immunohistochemistry staining (D1) and semi-quantitative data (D2). Data are expressed as mean ± SD of 3 independent experiments (n=6 in each group). *P<0.05 *vs* sham group fed with the same salt diet.

Supplemental Figure 4. High-salt-induced overexpression of AT1 receptors or Ang II is not observed in glial cells. Localization of central AT1 receptors or Ang II determined by double-staining with the antibodies against AT1 receptors or Ang II (green) and the antibody recognized glial fibrillary acidic protein (GFAP, red).

Supplemental Figure 5. Blockade of central RAS or oxidative stress inhibits salt-induced neuron activation in 5/6Nx rats. (A) Central administration of losartan or tempol and RDX or SDR attenuate activation of c-fos: representative photos of immunohistochemistry staining. (B) semi-quantitative data of immunohistochemistry staining. Data from 3 independent experiments are expressed as mean ± SD (n=6 in each group). *, P<0.05 *vs* 5/6Nx rats given vehicle.

Supplemental Figure 6. Blockade of central RAS, sympathetic signal, or oxidative stress inhibits salt-induced renal RAS activation in 5/6Nx rats. (A) The activity of ACE-1 in renal cortex. (B) Urinary AGT excretion. Data from 3 independent experiments are expressed as mean ± SD (n=6 in each group). *, P<0.05 *vs* 5/6Nx rats given vehicle.

Supplemental Table 1. Changes of circulating RAS and NE in the 5/6Nx rats with high-salt diet[A].

	Plasma AGT (ng/ml)		Serum ACE-1 activity (nmol/ml/min)		Plasma Ang Ⅱ (pg/ml)	
	0w	2w	0w	2w	0w	2w
IG Losartan (mg/kg/d)						
0	2920±138	2920±138	86±5	84±4	27±3	14±2
1	2911±297	2752±175	84±3	86±3	30±4	15±2
50	2886±207	2819±174	83±6	87±6	28±3	15±2
500	2908±208	2852±226	85±3	88±7	29±4	16±3
ICV Losartan (mg/kg/d)						
0	2958±205	2653±209	85±4	83±5	26±3	13±2
1	2848±267	2851±170	87±3	87±4	26±3	17±3
ICV Clonidine	2894±287	2799±195	86±6	86±4	27±5	16±3
RDX	2960±160	2786±196	85±5	87±5	25±4	18±4
SDR	2873±185	2692±201	84±4	86±5	27±3	15±4
ICV Tempol	2925±217	2831±186	86±5	88±7	26±4	16±2
IG Tempol	2917±264	2817±219	84±4	87±5	26±3	17±3
IG Hydralazine	2935±188	2761±163	85±6	84±3	28±5	15±4

[A]Data from 3 independent experiments are expressed as mean ± SD (n = 6 in each group); AGT, angiotensinogen; ACE-1, angiotensin-converting enzyme-1; Ang II, angiotensin II; ICV, intracerebroventricular injection; IG, intragastric gavage.

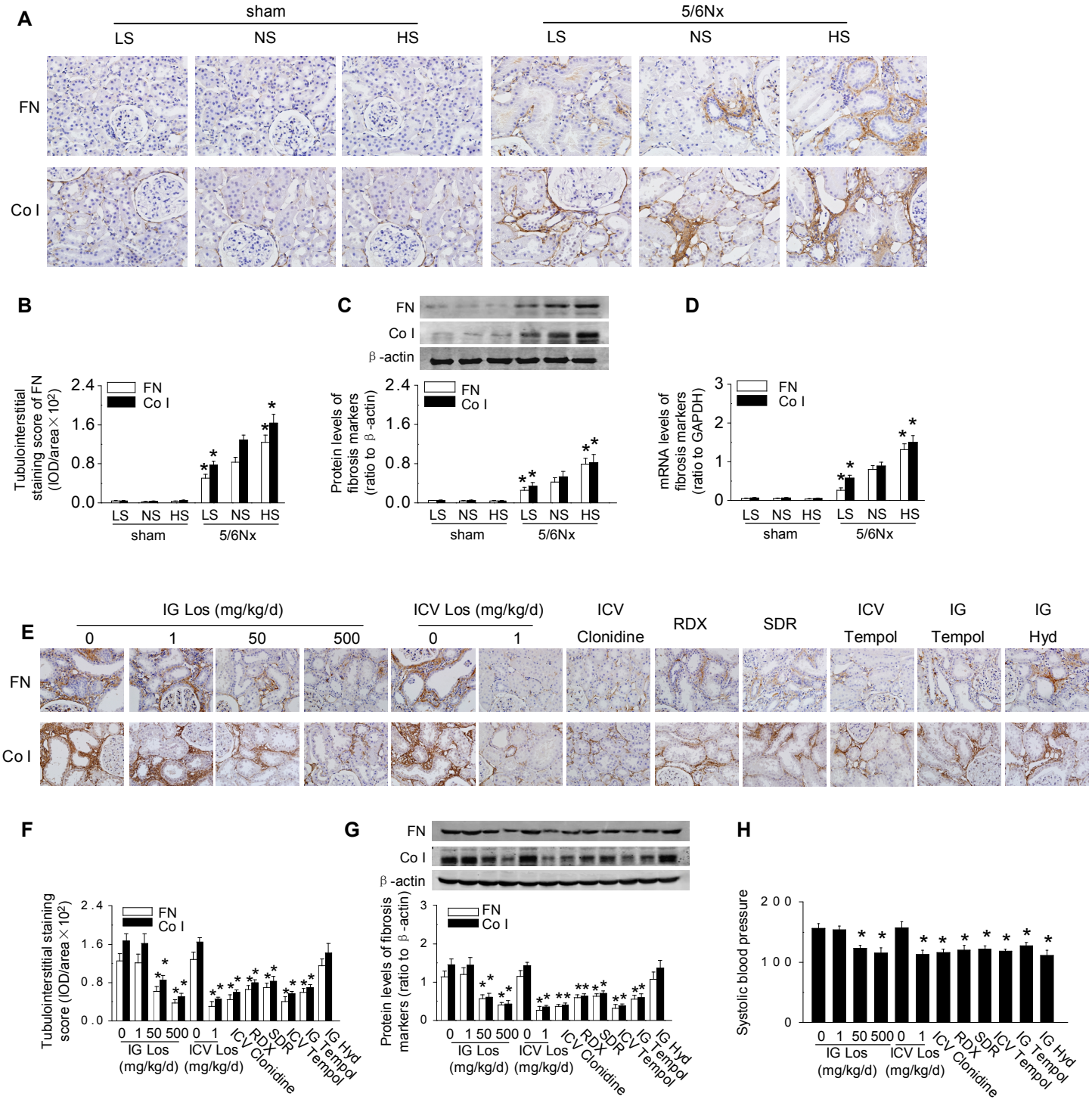

Supplemental Figure 1. High salt induces extracellular matrix accumulation in 5/6Nx rats.

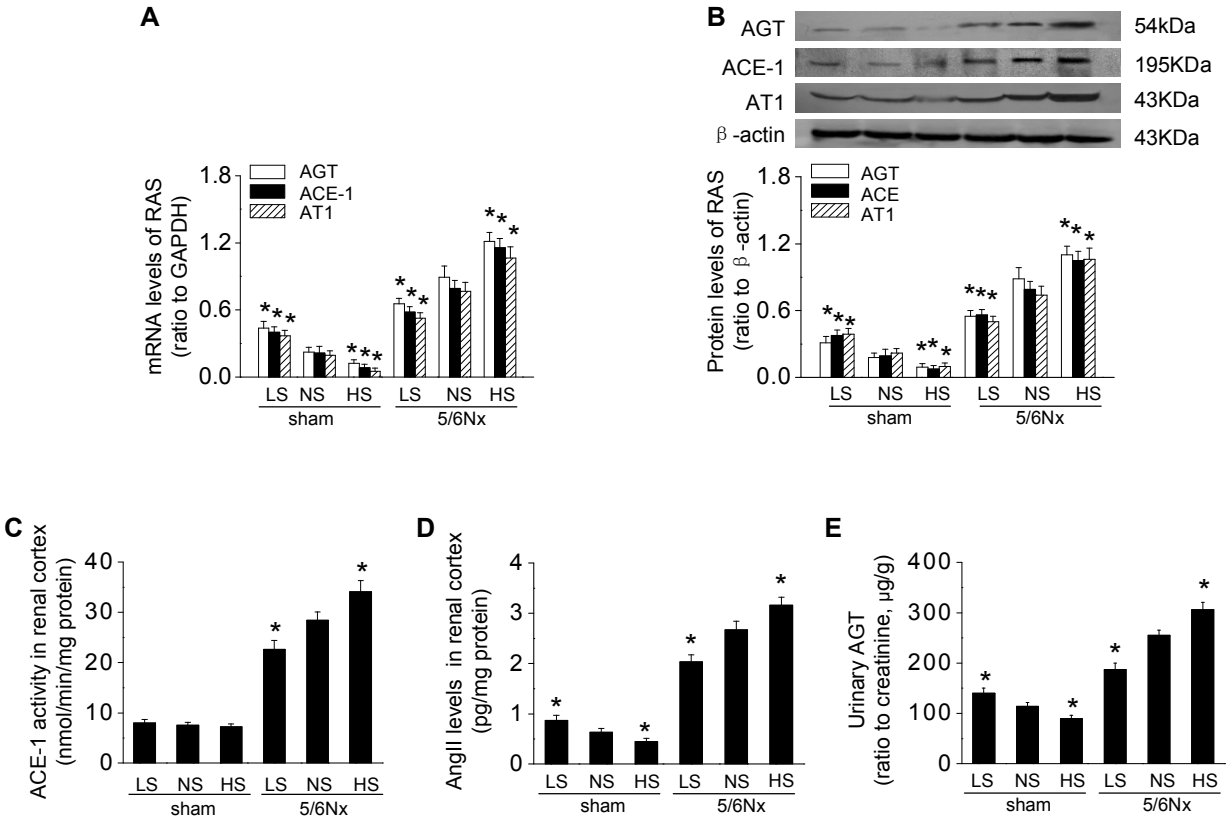

Supplemental Figure 2. High-salt intake activates intrarenal RAS in 5/6Nx rats.

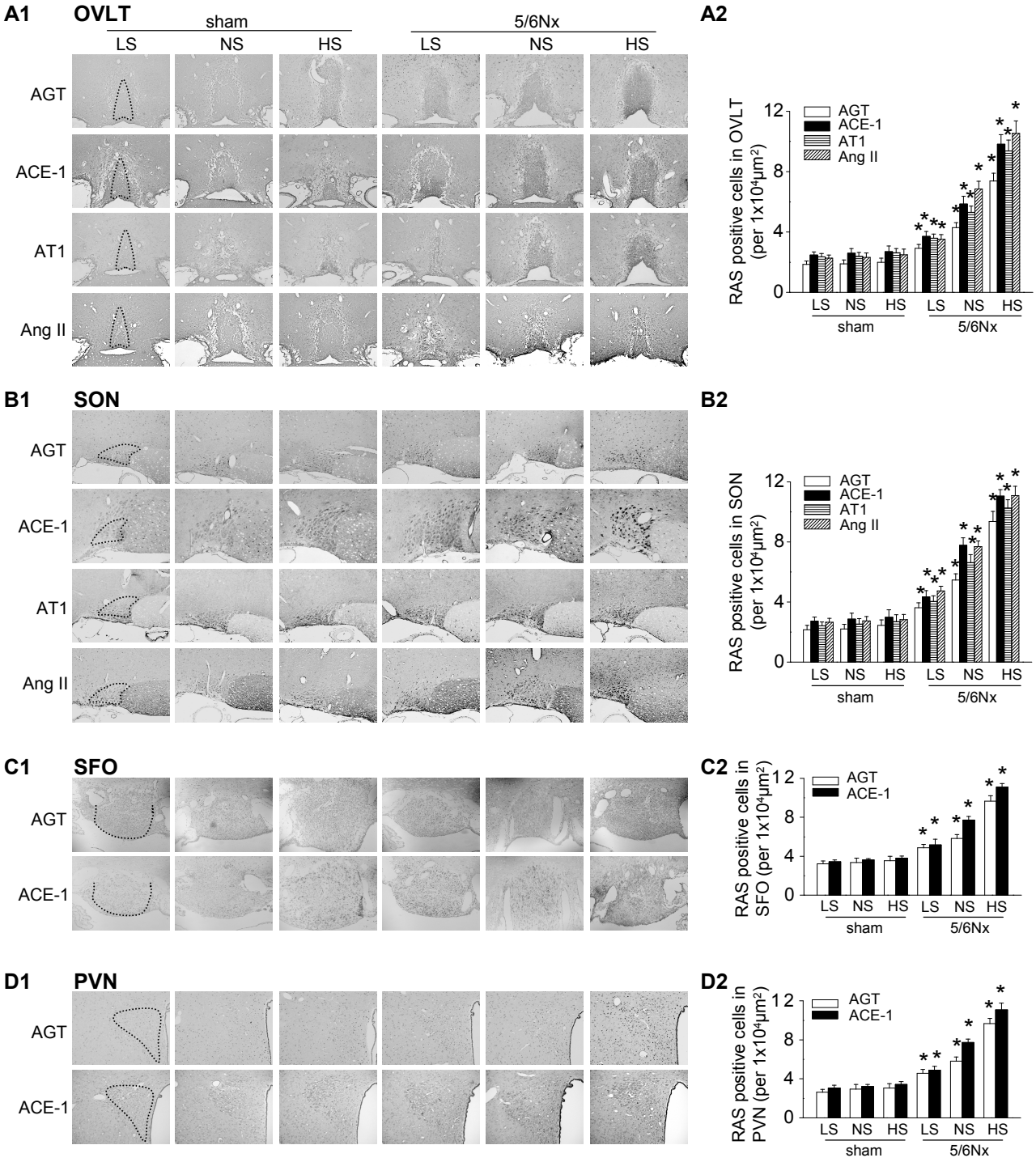

Supplemental Figure 3. High-salt intake unregulates expression of central RAS in brain organum vasculosum laminae terminalis and supraoptic nucleus in 5/6Nx rats.

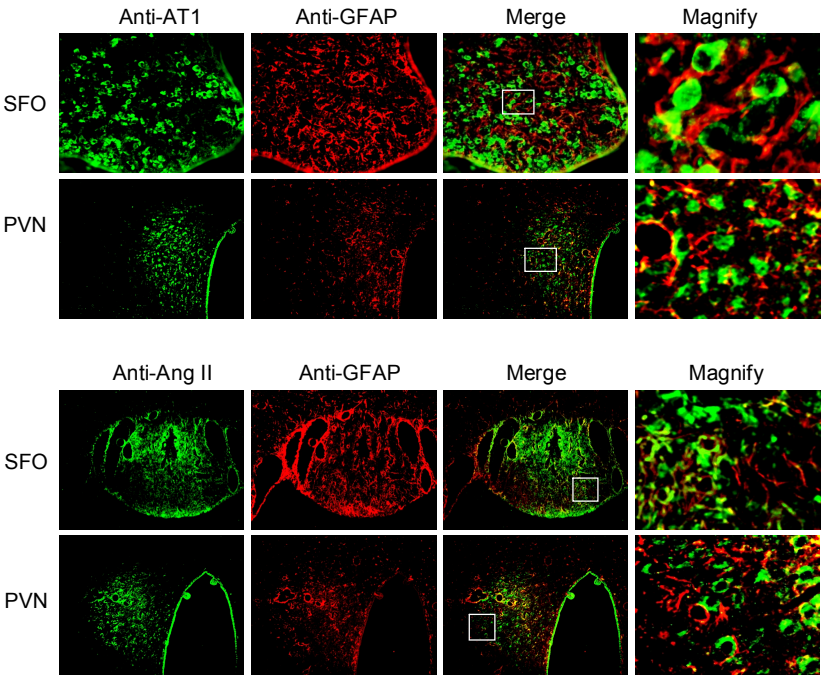

Supplemental Figure 4. High-salt-induced overexpression of AT1 receptors or Ang II is not observed in glial cells.

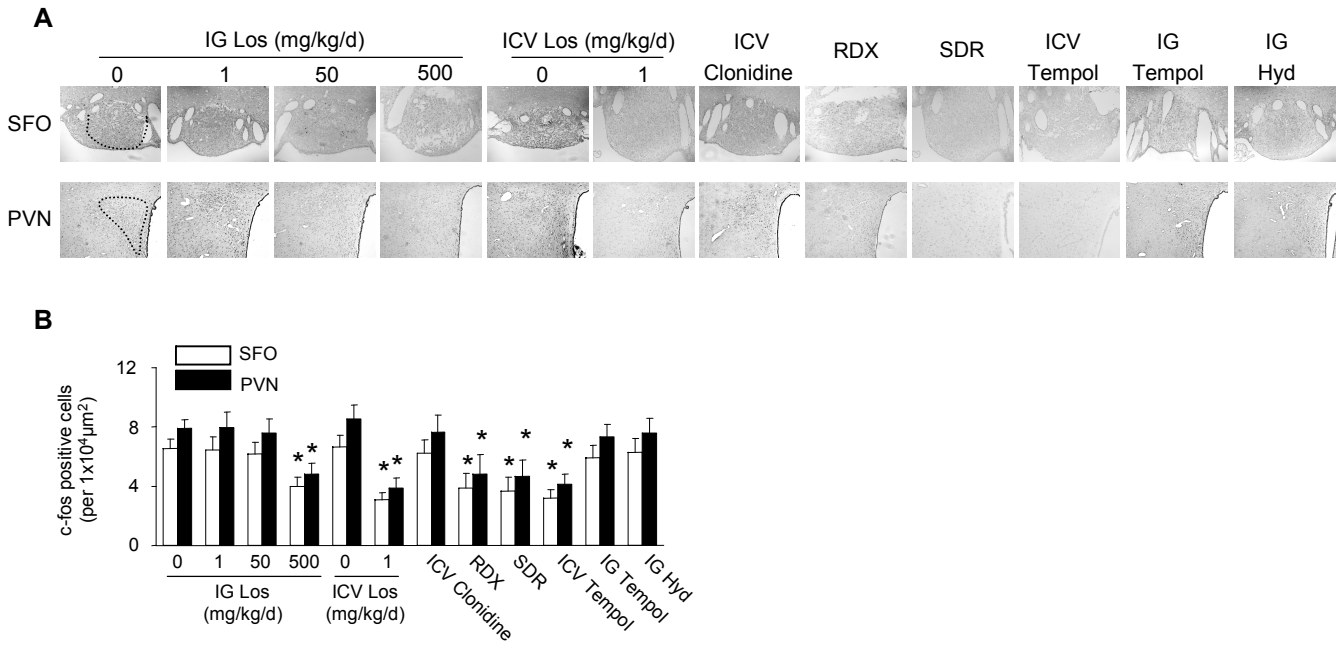

Supplemental Figure 5. Blockade of central RAS or oxidative stress inhibits salt-induced neuron activation in 5/6Nx rats.

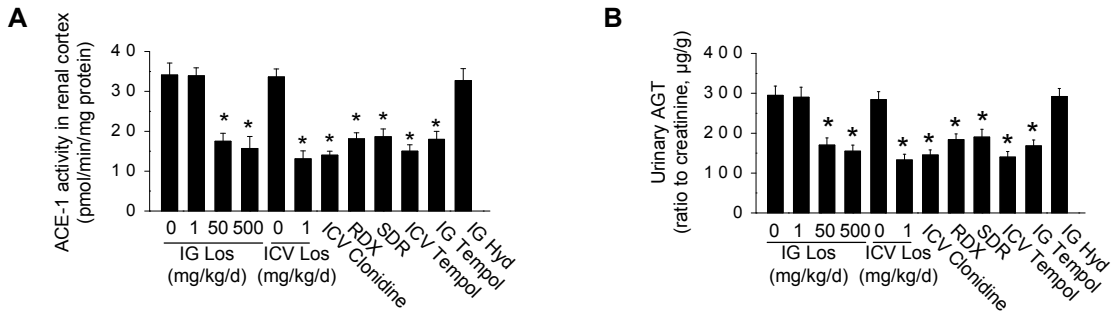

Supplemental Figure 6. Blockade of central RAS, sympathetic signal, or oxidative stress inhibits salt-induced renal RAS activation in 5/6Nx rats.